# Modeling Jump Diffusion in Zeolites: I. Principles and Methods[†]

Harikrishnan Ramanan[1] and Scott M. Auerbach[1,2,*]

*[1]Department of Chemical Engineering and [2]Department of Chemistry*
*University of Massachusetts, Amherst, MA 01003 USA*

## Abstract

We review the macroscopic variables relevant to single-component mass transfer through fixed zeolite particles or membranes. Through the Fick and Maxwell-Stefan formulations of diffusion, we relate these variables to transport coefficients calculable with molecular simulations. Using the Fick formulation, we discuss the diffusion-controlled and desorption-controlled limits of mass transfer. Through the well-known relation between the Fickian and Maxwell-Stefan diffusivities, we discuss expected temperature and loading dependencies in the limits of fluid-like and jump-like intrazeolite diffusion. We then review the statistical mechanical foundations of self-diffusion and Fickian- or transport-diffusion in terms of mean-square displacements. We outline how self-diffusion is influenced by kinetic correlations, geometrical correlations, vacancy correlations, single-file motion and disorder. For host-guest systems where guest motion is dominated by rare site-to-site jumps, we outline the use of transition state theory and kinetic Monte Carlo for constructing diffusion coefficients. We emphasize the particular difficulty in treating the competition between host-guest and guest-guest interactions when modeling rare event dynamics in zeolites.

[†]Submitted for the *Proceedings of the NATO Advanced Study Institute* on "Fluid Transport in Nanopores," Eds. J. Fraissard, W.C. Conner, Jr., and V. Skirda, La Colle Sur Loup, France, June 16-27, 2003.
[*]Address of correspondence: auerbach@samson.chem.umass.edu

## 1. Introduction

Knowledge of the mechanisms behind the reactivity and selectivity of zeolites and other microporous catalysts (in single-crystal as well as membrane forms) requires a detailed understanding of the mobility or the dynamical properties of adsorbed molecules within the microporous cavities of such materials. The separation mechanism exhibited by zeolite nanopores may be either: (a) "shape and size selectivity" (where molecular discrimination or screening occurs at the pore entrance or window due to the inability of one molecular type to access the porous network or transport pathway, e.g., $N_2$-$CH_4$ separation in ETS-4); (b) "interaction selectivity" (where separation occurs based on strong sorbate-zeolite interactions inside the pores, e.g., benzene-cyclohexane separation by Na-X); or (c) a complex interplay of (a) and (b). Though zeolites offer useful properties such as highly selective adsorption, diffusion and reaction, their small pore sizes and complex transport pathways provide significant resistances to molecular motion. One of the important goals in our research field is thus to *understand diffusion in zeolites to optimize the balance between high selectivity and high flux.* Detailed theoretical studies on two important zeolite types – MFI and FAU (Figure 1) have attributed their slow transport behavior to jump-like diffusion consisting of sequences of site-to-site jumps that are probabilistically rare [1, 2]. In this chapter, we explore the macroscopic phenomenologies and the microscopic mechanisms underlying jump diffusion in zeolites, with particular focus on revealing the temperature and loading dependencies of single-component fluid transport in nanopores.

The remainder of this chapter is organized as follows: In section II, we review various diffusion phenomenologies using language appropriate for membrane permeation. In section III, we discuss typical temperature and loading dependencies of transport coefficients controlling self- and transport diffusion, by comparing behaviors exhibited for jump-like and fluid-like motion. In section IV, we describe correlation functions that capture the microscopic bases of diffusion,

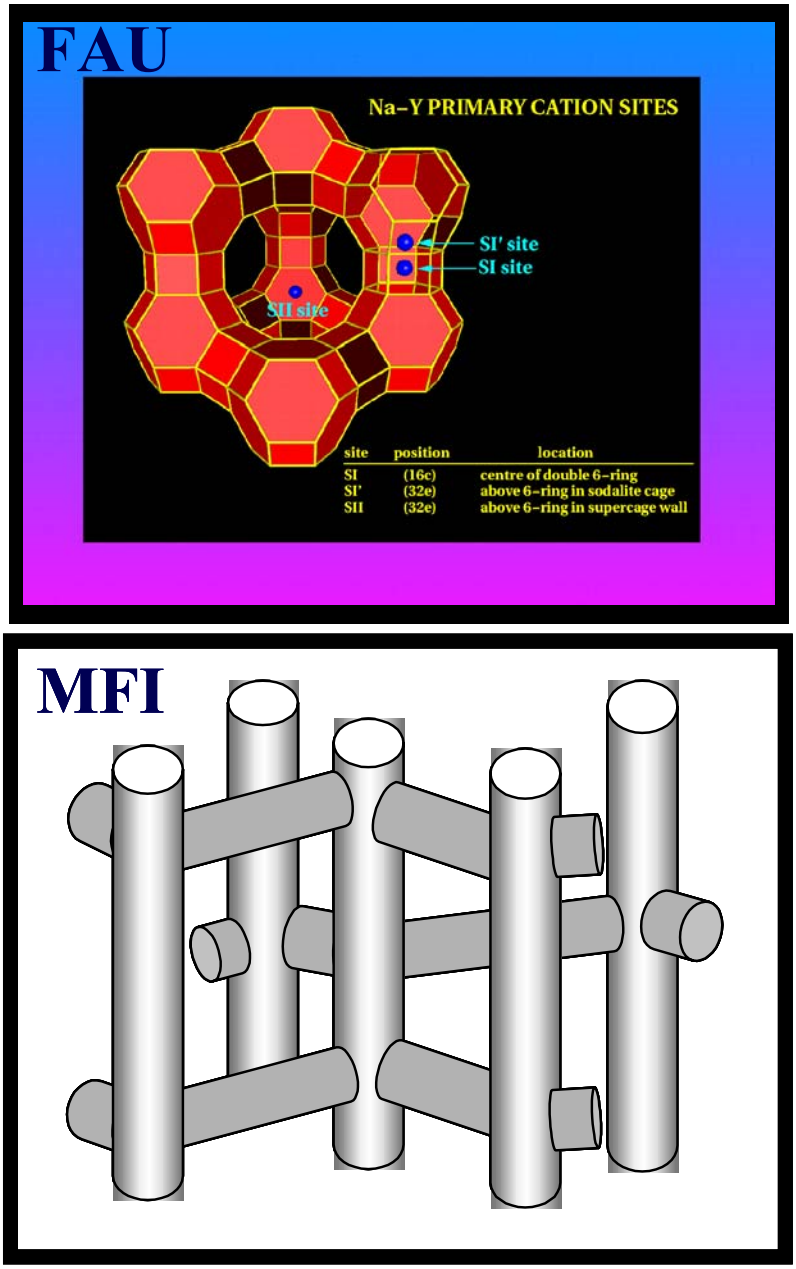


Figure 1: Two industrially important well-studied zeolite types – Faujasite (FAU) and Mobil–5 (MFI).

including kinetic, geometric and vacancy correlation effects. In section V, we outline transition state theory and kinetic Monte Carlo as simulation methods for modeling jump diffusion in zeolites. Finally, in section VI, we summarize the insights gained.

## 2. Diffusion Phenomenology:

### 2.1. Control and Response Variables

To discuss the phenomenology of diffusion, we consider the construction of the zeolite-guest system. Applications of zeolites typically do not restrict to the use of zeolite single crystals, but rather may also employ supported zeolite crystals that are closely inter-grown as a thin film or membrane. Figure 2 shows a 10 μm thick cross-section of a siliceous MFI-type membrane as an example. Zeolite membranes are (nowadays) typically formed from myriad closely assembled

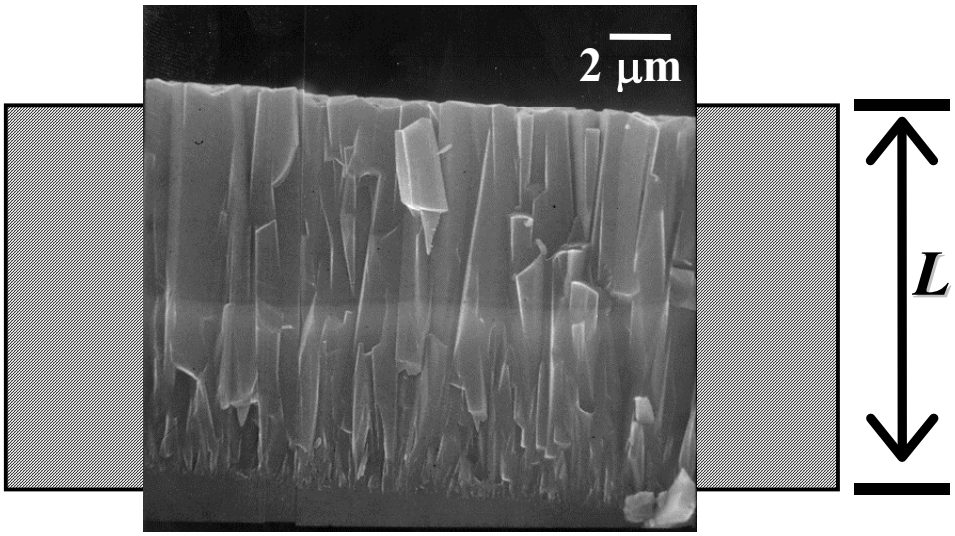


Figure 2: Cross-sectional view of a typical zeolite membrane of thickness L (Inset shows the Scanning electron microscope image of an MFI membrane as an example).

micro-crystallites [3, 4]. By guest or sorbate diffusion through the membrane, we mean transport through the microporous zeolite structure. Here we explore the macroscopic system parameters that control steady-state permeation through such zeolite membranes. Towards that end, we pose the following questions:

(a) What macroscopic variables do we *control*?

(b) What are the *responses* to those controls?

(c) How are the controls and responses *related*?

Permeation through zeolite membranes is controlled by: the choice of *zeolite* (host), *sorbate* (guest) and the *process conditions* under which permeation takes place. Regarding the zeolite, we can choose framework topology, chemical composition of the framework (e.g., the Si:Al ratio), and membrane thickness. Regarding the adsorbed guest phase, we may choose the molecular size, shape and polarity. Process variables include temperature ($\boldsymbol{T}$) , inflow pressure ($\boldsymbol{P}_{hi}$) and outflow pressure ($\boldsymbol{P}_{lo}$). Pressures are typically used to specify external fluid-phase activities because adsorption in zeolites is relatively strong; so much so that near-complete pore filling can often be achieved by placing zeolites in contact with relatively dilute vapors.

In addition to these standard control variables, we note that recent progress has been made in controlling the microstructures of zeolite membranes[4]. For example, by modifying membrane synthesis conditions, Tsapatsis and coworkers have fabricated both b-oriented and c-oriented MFI membranes[5]. The crucial point is – In order to comprehend complete insight in diffusion in zeolites, it is not enough to know the zeolite type, composition and particle size; one must also have a sense how the zeolite was actually synthesized.

Here we address the macroscopic responses to the control variables discussed above. In general, experimentalists monitor either the transient uptake rate or the steady-state flux. We focus on the latter, being more relevant to membrane permeation measurements (Figure 3A). The flux is defined by:

Flux through the membrane = Mass/Time/Area

= Density * Velocity

$\equiv \boldsymbol{J}$ (moles/s/m$^2$ or kg/hr/m$^2$) (1)

By defining the flux on a 'per area' basis, the flux becomes independent of area in analogy with pressure (force per area). Two other variables that are often used to report permeation data are the permeance and the permeability coefficient, defined according to:

Permeance through the membrane = Flux/Pressure drop

$= \boldsymbol{J}/(\boldsymbol{P}_{hi} - \boldsymbol{P}_{lo})$ (2)

Permeability Coefficient = Permeance * Membrane thickness

$= \boldsymbol{J}*\boldsymbol{L}/(\boldsymbol{P}_{hi} - \boldsymbol{P}_{lo})$ (3)

The permeance becomes useful in the "Henry's law" adsorption regime, i.e., at low pressures where loadings are low, because in this regime the permeance is independent of pressure drop. The permeability coefficient becomes useful in the "diffusion-limited" transport regime, i.e., for relatively thick membranes (*vide infra*), because in this regime the permeability coefficient is independent of membrane thickness.

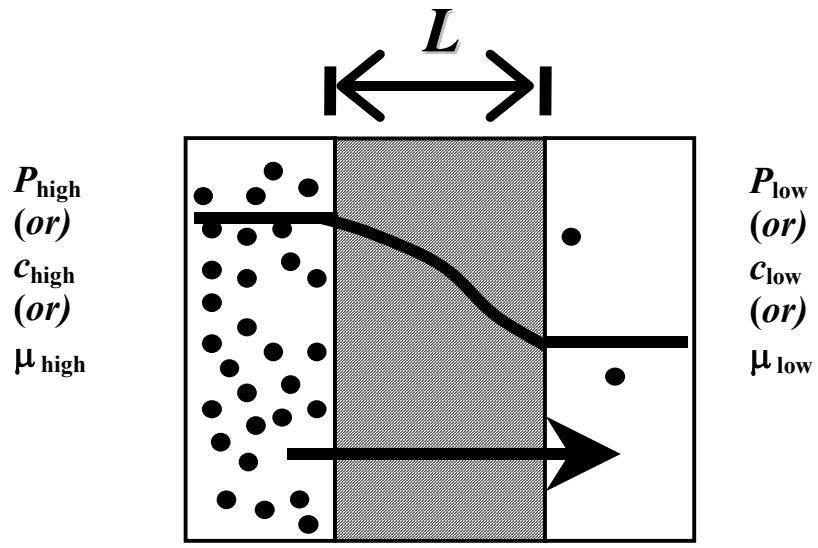


Figure 3A: Schematic of a permeation experiment through a zeolite membrane of thickness L (Diffusion driving force expressed in three different forms, i.e, $-\nabla \boldsymbol{P}$, $-\nabla \boldsymbol{c}$ and $-\nabla \boldsymbol{\mu}$.

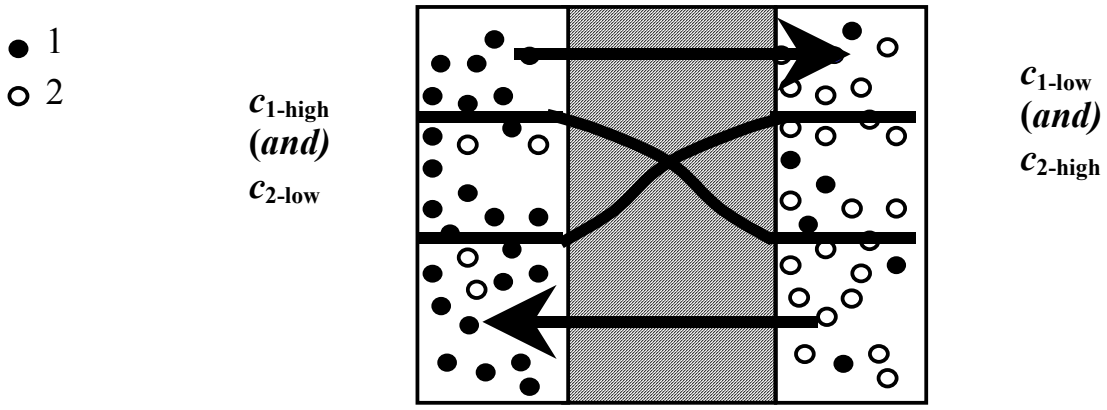


Figure 3B: Schematic of an equimolar counter-diffusion experiment through a zeolite membrane.

If these considerations hold, we have that:

$$\text{Constant} = J^{*}L/(P_{hi} - P_{lo}) \quad (4a)$$

$$\Rightarrow J \propto \nabla P \text{ (If linear pressure-drop is considered)} \quad (4b)$$

$$\Rightarrow J = -\wp \nabla P + O(\nabla P^2). \quad (4c)$$

Here $\nabla P$ is a "driving force" in the sense that if $\nabla P$ were zero, the flux would vanish. $J$ is the response to the driving force $\nabla P$, and $\wp$ (the permeability coefficient) is the constant of proportionality. If terms of order $\nabla P^2$ can be ignored, the system is in the "linear response" regime. Otherwise, we ought to consider explicitly such higher-order terms. Instead, most transport formulations eschew explicit reference to higher-order driving forces, preferring to sweep these effects into a "loading dependence" of the transport coefficient $\wp$. As such, our first diffusion phenomenology, i.e., a mathematical equation connecting control and response variables, takes the form:

$$J = -\wp \nabla P. \quad (5)$$

Other more useful phenomenologies exist for diffusion, based on concentration gradients and chemical potential gradients, the pros and cons of which are discussed below. In terms of the concentration gradient $\nabla c$ across the membrane, we have Fick's law that takes the form:

$$J = -D \nabla c + O(\nabla c^2), \quad (6)$$

where $D$ is the Fickian or transport diffusion *constant*, with units of length squared per time. Folding higher-order effects into $D$ produces the Fickian diffusion *coefficient* $D(c)$ (i.e., no longer constant), which depends on the local sorbate concentration in the membrane. As such, Fick's law takes the form:

$$\boldsymbol{J} = -\boldsymbol{D}(\boldsymbol{c})\nabla \boldsymbol{c} \tag{7}$$

The great value of Fick's law is its connection with the continuity equation, which expresses the conservation of mass according to:

$$\frac{\boldsymbol{dc}}{\boldsymbol{dt}} = -\nabla \cdot \boldsymbol{J} \tag{8}$$

Plugging Fick's flux into the equation above gives the "diffusion equation" also know as Fick's second law:

$$\frac{\boldsymbol{dc}}{\boldsymbol{dt}} = \nabla \cdot \left(\boldsymbol{D}(\boldsymbol{c})\nabla \boldsymbol{c}\right) \tag{9}$$

Note that in general, $\boldsymbol{D}(\boldsymbol{c})$ depends implicitly on space through its concentration dependence, requiring it to remain sandwiched between the two gradient operators. Solving this and related differential equations for various physically-motivated boundary conditions has been the focus of attention for many years.

In principle, Fick's law can be generalized for multi-component systems according to:

$$\boldsymbol{J}_i = -\sum_j \boldsymbol{D}_{ij} \nabla \boldsymbol{c}_j \tag{10}$$

However, when equation (10) is used to interpret experimental data for complex transport systems, one finds the possibility that $\boldsymbol{D}_{ij}$ can become *negative* [6], suggesting that other formulations of multi-component transport are required. Nevertheless, equation (10) becomes useful for interpreting a very special kind of multi-component system, involving equimolar counter-permeation of identical but labeled particles, also known as "tracer counter-permeation" and more generally as self-diffusion[7]. This situation, shown in Figure 3B, is characterized by the following diffusion phenomenologies:

$$\boldsymbol{J}_1 = -\boldsymbol{D}_s \nabla \boldsymbol{c}_1 + \boldsymbol{O}(\nabla \boldsymbol{c}_1^2) \tag{11a}$$

$$\boldsymbol{J}_2 = -\boldsymbol{D}_s \nabla \boldsymbol{c}_2 + \boldsymbol{O}(\nabla \boldsymbol{c}_2^2). \tag{11b}$$

Here $\boldsymbol{D}_s$ is the self-diffusion constant, also with units of length squared per time. Again, folding higher-order effects into $\boldsymbol{D}_s$ gives the self-diffusion coefficient, which we expect to be lower than the single-component Fickian $\boldsymbol{D}(\boldsymbol{c})$, because self-diffusion involves counter-flow and hence greater transport resistance. Taking into account the equal and opposite fluxes in self-diffusion suggests adding equations (11a) and (11b) to yield:

$$\boldsymbol{J}_1 + \boldsymbol{J}_2 = \boldsymbol{0} \Rightarrow \nabla \boldsymbol{c}_1 + \nabla \boldsymbol{c}_2 = \boldsymbol{0} = \nabla \boldsymbol{c}_{\text{total}}. \tag{12}$$

Therefore, in self-diffusion the total concentration of both components is constant through the membrane, suggesting that $\boldsymbol{D}_s$ depends upon $\boldsymbol{c}_{\text{total}}$, the total concentration of both components. As such, self-diffusion is an equilibrium property of the system. Combining self-diffusive flux with the law of conservation of mass, i.e., equation (8), we get the self-diffusion equation:

$$\frac{\boldsymbol{dc}}{\boldsymbol{dt}} = \boldsymbol{D}_s \nabla^2 \boldsymbol{c} \tag{13}$$

where, $\boldsymbol{c}(\boldsymbol{r},\boldsymbol{t})$ is the position and time dependent concentration of labeled molecule(s). Solving equation (13) with a "Delta-function" initial condition, $\boldsymbol{c}(\boldsymbol{r},\boldsymbol{t})$ is found to be proportional to the "propagator" or the probability distribution of molecular displacements at $(\boldsymbol{r},\boldsymbol{t})$, i.e.,

$$\boldsymbol{c}(\boldsymbol{r},\boldsymbol{t}) \propto \boldsymbol{e}^{-\frac{\boldsymbol{r}^2}{4\boldsymbol{D}_s \boldsymbol{t}}} \tag{14}$$

The mean-square displacement is obtained as the second moment of this probability distribution; this yields the "Einstein equation:"

$$\left\langle \boldsymbol{r}^2(\boldsymbol{t}) \right\rangle = 6\boldsymbol{D}_s \boldsymbol{t}\,. \tag{15}$$

In what follows, we omit explicit references to higher-order driving-force terms, understanding that these are folded into concentration dependencies of transport coefficients.

The obvious importance of understanding multicomponent diffusion in zeolites, coupled with the challenge this phenomenon poses to the Fickian formulation, warrants the development of new diffusion formulations. Most of these replace the concentration-based driving force with chemical potential gradients ($\nabla\mu$). Such a replacement is physically attractive for several reasons. First, the chemical potential gradient can be regarded as an actual force (energy/length), albeit a thermodynamic one, facilitating its use in force-balance equations (*vide infra*). Second, chemical potential gradients are recognized as the true drivers of diffusive mass transport. Indeed, experimental data confirms that diffusion ceases when chemical potential gradients vanish, even if concentration gradients persist [8].

Here we discuss the Onsager and Maxwell-Stefan formulations of diffusion. The Onsager approach resembles the Fickian formulation, except for the $\nabla c \rightarrow \nabla\mu$ substitution. The multicomponent version takes the form:

$$\boldsymbol{J}_i = -\sum_j \boldsymbol{L}_{ij} \nabla \mu_j \qquad (16)$$

where $\boldsymbol{L}_{ij}$ and $\nabla\mu_j$ are concentration-dependent Onsager transport coefficients and local chemical potential gradients, respectively. The coefficients $\boldsymbol{L}_{ij}$ have units of flux/force, and are related to important statistical mechanical correlation functions. Recent molecular dynamics (MD) simulations of these correlation functions suggest that all these $\boldsymbol{L}_{ij}$'s are positive, which already represents progress from the Fickian approach [9]. A disadvantage of the Onsager approach is that the coefficient $\boldsymbol{L}_{ij}$ is influenced by both guest($\boldsymbol{i}$)-guest($\boldsymbol{i}$) and guest($\boldsymbol{i}$)-guest($\boldsymbol{j}$) interactions, making its physical interpretation more complicated. In practice, simulators calculate Onsager coefficients

directly from MD or kinetic Monte Carlo (KMC) simulations; these parameters are then transformed to Fickian diffusivities for use in reaction-diffusion equations [9].

An alternative approach based on chemical potential gradients succeeds in disentangling the guest(***i***)-guest(***i***) and guest(***i***)-guest(***j***) interactions. This is the Maxwell-Stefan formulation, which was originally developed for multi-component diffusion in bulk fluids. This approach has since been generalized by Krishna to multi-component surface diffusion [6], and has been applied with great skill to diffusion in zeolites by Krishna and coworkers [10]. While Fick and Onsager postulate phenomenological flux expressions, Maxwell and Stefan balance diffusive and drag forces. For single-component transport driven by a chemical potential gradient across a membrane (Figure 3A), the Maxwell-Stefan equation takes the form:

$$-\nabla\boldsymbol{\mu} = \boldsymbol{RT}\frac{\boldsymbol{\nu}}{\boldsymbol{D}^{\boldsymbol{MS}}} \tag{17}$$

where $\boldsymbol{D}^{\boldsymbol{MS}} = \boldsymbol{D}^{\boldsymbol{MS}}(\boldsymbol{c})$ is the concentration-dependent Maxwell-Stefan (MS) surface diffusion coefficient, $\boldsymbol{\nu}$ is the macroscopic velocity of the permeating phase, and $RT/\boldsymbol{D}^{MS}$ is a friction coefficient representing the effective drag experienced as the adsorbed phase permeates through the zeolite membrane. Here, the diffusion driving force is the negative of the chemical potential gradient. This phenomenology can be generalized for multi-component systems by adding a drag term for each additional component to the drag exerted by single-component zeolite-guest systems. For example, the transport of a binary mixture of permeating components (1 and 2) is described by:

$$-\nabla\boldsymbol{\mu}_1 = \boldsymbol{RT}\frac{\boldsymbol{\nu}_1}{\boldsymbol{D}_1^{\boldsymbol{MS}}} + \boldsymbol{RTx}_2\frac{(\boldsymbol{\nu}_1 - \boldsymbol{\nu}_2)}{\boldsymbol{D}_{12}^{\boldsymbol{MS}}} \tag{18}$$

where $\boldsymbol{D}_{12}^{MS} = \boldsymbol{D}_{12}^{MS}(\boldsymbol{c})$ denotes the loading-dependent binary MS diffusivity corresponding to the interaction between components 1 and 2; $\boldsymbol{D}_{1}^{MS}(\boldsymbol{c})$ remains the MS surface diffusivity of component 1 relative to the zeolite membrane. In principle, $\boldsymbol{D}_{1}^{MS}(\boldsymbol{c})$ for the multi-component mixture may be different from that for the single-component case. In practice, though, it is found that the behavior, e.g., loading dependence, of $\boldsymbol{D}_{1}^{MS}(\boldsymbol{c})$ is largely unchanged when adding additional sorbed phases. This is one of the great advantages of the Maxwell-Stefan approach to multi-component transport problems. The Maxwell-Stefan approach also provides an elegant formulation of self-diffusion, which is a multi-component process from a macroscopic standpoint.

Although the Maxwell-Stefan approach succeeds at formally disentangling ***i-i*** and ***i-j*** interactions by defining $\boldsymbol{D}_{1}^{MS}(\boldsymbol{c})$ and $D_{12}^{MS}(c)$, a direct statistical mechanical calculation of $D_{12}^{MS}(c)$ remains elusive, in contrast to Onsager's $\boldsymbol{L}_{ij}$. An empirical approach for determining $D_{12}^{MS}(c)$, adapted by Krishna from bulk-fluid applications, involves logarithmic interpolation of single-component Maxwell-Stefan surface diffusivities [6]. This Maxwell-Stefan-Krishna approach has been shown to reproduce multi-component sorption kinetics with only single component diffusion data, augmented with multi-component adsorption isotherm data [10].

## 2.2. Relationship between Fick and Maxwell-Stefan Diffusivities

Here we show how to connect the Fickian and Maxwell-Stefan approaches, i.e., how to relate the single-component diffusivities, by equating fluxes from the two formulations. Beginning with the *ansatz* of Fick and Maxwell-Stefan, i.e.:

$-\nabla\boldsymbol{\mu} = \boldsymbol{RT}\dfrac{\boldsymbol{v}^{MS}}{\boldsymbol{D}^{MS}}$ and $\boldsymbol{J}_{Fick} = \boldsymbol{cv} = -\boldsymbol{D}_{Fick}\nabla\boldsymbol{c}$ , we find that:

$$\boldsymbol{J}_{Fick} = \boldsymbol{J}_{MS} \tag{19a}$$

$$-\boldsymbol{D}_{Fick}\nabla \boldsymbol{c} = -\frac{\boldsymbol{D}^{MS}}{\boldsymbol{RT}}\boldsymbol{c}\nabla\boldsymbol{\mu} = -\frac{\boldsymbol{D}^{MS}}{\boldsymbol{RT}}\boldsymbol{RT}\Gamma\nabla\boldsymbol{c} = -\boldsymbol{D}^{MS}\Gamma\nabla\boldsymbol{c} \tag{19b}$$

$$\boldsymbol{D}_{Fick} = \boldsymbol{D}^{MS}\Gamma \tag{19c}$$

Here, the term $\Gamma$ is referred to as the thermodynamic correction factor expressed as:

$$\Gamma = \left(\frac{\partial \ln \boldsymbol{f}}{\partial \ln \boldsymbol{c}}\right)_{T} \tag{19d}$$

where $\boldsymbol{f}$ is the fugacity of the bulk fluid phase and $\boldsymbol{c}$ is the loading in the sorbent. Hence, $\Gamma$ can be evaluated from equilibrium sorption isotherm data for the sorbate. The Fick diffusivity is therefore a composite of diffusive effects ($\boldsymbol{D}^{MS}$) and thermodynamic effects ($\Gamma$). This perspective is buoyed from the diffusive properties of bulk fluids, which tend to show Maxwell-Stefan diffusivities with mild loading dependences [6]. Therefore, much of the loading dependence of the Fick diffusivity actually arises from the loading dependence of $\Gamma$. This understanding has been extended to systems that exhibit weak zeolite-guest interactions (e.g. methane in silicalite [11]). The MS diffusivity has also been called the "corrected diffusivity." This becomes a particularly useful designation when both $\boldsymbol{D}_{\text{Fick}}$ and $\Gamma$ are experimentally measured, and $\boldsymbol{D}_{\text{Fick}}/\Gamma$ is found to have a much weaker loading dependence than does $\boldsymbol{D}_{\text{Fick}}$. Hence, the "correction" means that the thermodynamically induced loading dependence in $\boldsymbol{D}_{\text{Fick}}$ has been removed.

We close this section with some final comments on equation (19c). When the sorbate loading is low the thermodynamic factor is nearly unity, indicating that for nearly ideal systems the Fickian and Maxwell-Stefan diffusivities agree. They differ at higher sorbate loadings because of the different ways that the loading-dependencies of the Fick and Maxwell-Stefan diffusivities fold

higher-order effects into pseudo-linear-response relations. Several researchers approximate equation (19c) by replacing the Maxwell-Stefan diffusivity with the self-diffusion coefficient, because the latter can be obtained under purely equilibrium conditions. Equation (19c) under such an approximation is often called the Darken equation. Unfortunately, some authors also call equation (19c) itself the Darken equation. Beware!

## 2.2. Diffusion- vs. Desorption-limited Flux

Having discussed macroscopic phenomenologies of diffusion, we now address the following microscopic questions:

(a) What microscopic processes control fluxes?

(b) How do diffusion and desorption rates combine to produce overall flux?

(c) What experimental methods exist to determine which process controls the flux?

Answering these questions requires a microscopic model of membrane permeation. For pedagogical purposes, we choose the simplest possible model that embodies the spirit of diffusion in zeolites, which often involves cage-to-cage and site-to-site jump motions. In particular, we choose a two-dimensional square lattice of identical adsorption sites, i.e., a Langmuirian host-guest system [12] as shown in Figure 4A. Variants of this model have been developed that produce accurate simulations of diffusion in zeolites, when parameterized by transition state theory calculations and evolved using kinetic Monte Carlo simulations (*vide infra*) [1]. Adsorption sites are represented in Figure 4A as squares, molecule A as dark-shaded circles and molecule B as light-shaded circles. A schematic energy diagram for adsorbed guests is shown in Figure 4B, as a function of position along the membrane thickness.

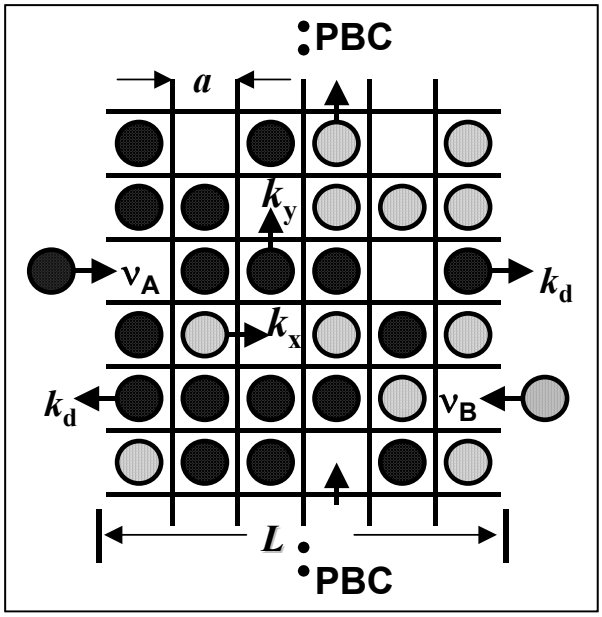


Figure 4A: Langmuirian host-guest model representation of a membrane permeation system: Two-dimensional square lattice showing cross-diffusion phenomena.

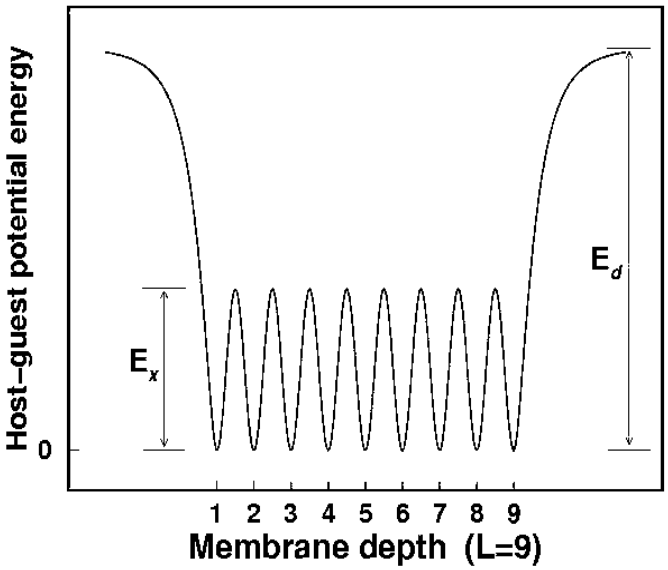


Figure 4B: Langmuirian host-guest model representation of a membrane permeation system: Potential energy diagram for lattice sites along the depth of membrane.

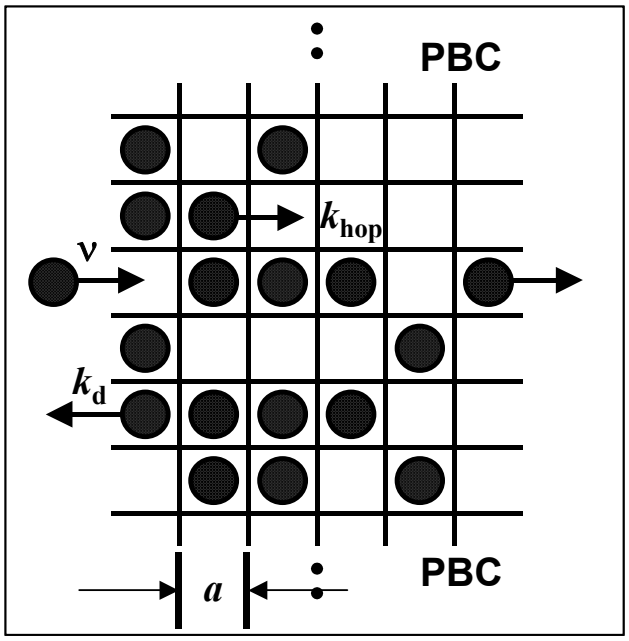


Figure 4C: Langmuirian host-guest model representation of a membrane permeation system: Lattice model showing steady-state flux into vacuum.

The model is defined by the following parameters: (a) the potential energy decrease for a molecule to change its position from outside the lattice to an adsorption site is $E_d$ (energy of adsorption); (b) rate at which **A** molecules attempt to enter the lattice from the fluid phase is given by the frequency $\nu$, (c) rate of desorption is $k_d$; (d) rates of molecular hops from one adsorption site to another in the **x** and **y** directions are $k_x$ and $k_y$, respectively; and (e) the site-to-site distance is **a**.

The basic model assumptions are: (a) the differential heat of sorption is independent of sorbate loading, i.e., sites are energetically uncoupled from each other; (b) molecular jumps from an occupied site to an adjacent vacant site are temporally uncorrelated and require surmounting an energy barrier; and (c) guest-guest interactions are ignored with the exception that attempted jumps to occupied sites are unsuccessful, as dual occupancy is not permitted.

This model incorporates both host-guest and guest-guest potential interactions through rare site-to-site jumps and site blocking, respectively. Studies on single-file diffusion in zeolite membranes can be carried out using this model by considering the special case: $\frac{\boldsymbol{k}_y}{\boldsymbol{k}_x} \to 0$ [13]. And, of course, this model reveals the competition between rates of diffusion and desorption.

On the other hand, the Langmuirian model ignores a variety of specialized phenomena. The model in its simplest form does not include guest-guest attractions or associations, although we have augmented it to treat these effects [14]. The model ignores cooperative motion [15], and is rather inconvenient for studying temperature- and loading-dependent lattice motion.

We now explore three consequences of the Langmuirian host-guest model pertaining to (*i*) fractional loading, (*ii*) adsorption isotherms and (*iii*) transport diffusion. First, partitioning intra-membrane volume into discrete sites suggests a new concept of concentration called the fractional loading, $\boldsymbol{\theta}$. In particular, the concentration, $\boldsymbol{c}$ (number of adsorbates/volume adsorbent) takes the form:

$\boldsymbol{c}$ = (Number of adsorbates $\boldsymbol{n}$)/(Total number of sites $\boldsymbol{n}_{\text{sites}}$ × volume per site $\boldsymbol{v}_{\text{site}}$)

$= (\boldsymbol{n}/\boldsymbol{n}_{\text{sites}}) \times (1/\boldsymbol{v}_{\text{site}})$

$\equiv \quad (\boldsymbol{\theta}) \quad \times \quad (\boldsymbol{c}_{\max}) \Rightarrow \boldsymbol{J} = -\boldsymbol{D}\nabla\boldsymbol{c} = -\boldsymbol{c}_{\max}\boldsymbol{D}\nabla\boldsymbol{\theta} = -\boldsymbol{D}\nabla\boldsymbol{\theta}$ (if $\boldsymbol{v}_{\text{site}} \equiv 1$) (20)

Second, the Langmuir adsorption isotherm can be derived by equating adsorption and desorption fluxes, according to:

$$\boldsymbol{J}_{adsorption} = \boldsymbol{J}_{desorption} \tag{21a}$$

i.e., $\boldsymbol{\nu}(1-\boldsymbol{\theta}) = \boldsymbol{k}_d\boldsymbol{\theta}$; where $\boldsymbol{\nu} \propto \boldsymbol{p}/\sqrt{\boldsymbol{T}}$ (21b)

$$\Rightarrow \theta_{eq} = \frac{\nu}{\nu + k_d} = \frac{1}{1 + \frac{k_d}{\nu}} = \frac{1}{1 + \frac{b}{p}} \text{ where } b \propto k_d\sqrt{T} \quad (21c)$$

Third, the simple Fickian diffusion phenomenology implied by equation (6), i.e., where $D$ is independent of concentration, arises for Langmuirian systems *without higher-order terms even at maximal loadings* [16]. The single-component Fickian diffusivity for Langmuirian systems takes the form: $D_0 = k_{hop}a^2$. As a consequence, the concentration profile is linear in the direction of motion at steady state.

For the special case of steady-state membrane flux from a high-pressure side to vacuum (Figure 4C), we obtain a formula for the flux by equating the fluxes from the left edge, right edge, and membrane interior according to:

Left edge flux ($J_L$) = Middle flux ($J_M$) = Right edge flux ($J_R$)

$$J_L = \nu(1 - \theta_L) - k_d\theta_L \quad (22a)$$

$$J_M = -D_0 \frac{(\theta_R - \theta_L)}{L} \text{ as } \nabla\theta = \text{constant} \quad (22b)$$

$$J_R = k_d\theta_R \quad (22c)$$

Solving for the 2 unknowns ($\theta_L$ and $\theta_R$) from 2 steady state equations, we have

$$J = -\frac{k_d\theta_{eq}D_0}{k_dL + D_0(2 - \theta_{eq})} \quad (22d)$$

Two important limiting conditions can be identified, keeping in mind that $(2-\theta_{eq})$ remains of order unity. These limits are:

(a) For $k_d L \gg D_0$, $J = \dfrac{\theta_{eq} D_0}{L} \Rightarrow$ diffusion-controlled process (22e)

(b) For $k_d L \ll D_0$, $J = k_d \theta_{eq} \Rightarrow$ desorption-controlled process (22f)

By testing the $L$-dependence of flux across membranes of various known thicknesses, we can determine if steady-state permeation is diffusion- or desorption-controlled.

Because zeolite membranes are typically few tenths of a micron thick, it is usually assumed that zeolite permeation is diffusion-controlled. Equation (22e) can thus be used to predict the temperature-dependence of flux for a given pressure, by knowing the temperature-dependencies of $\theta_{eq}$ and $D_0$. This is shown in Figure 5 from model studies on single-component permeation through Langmuirian membranes [17]. Figure 5 shows that the flux increases with temperature at relatively

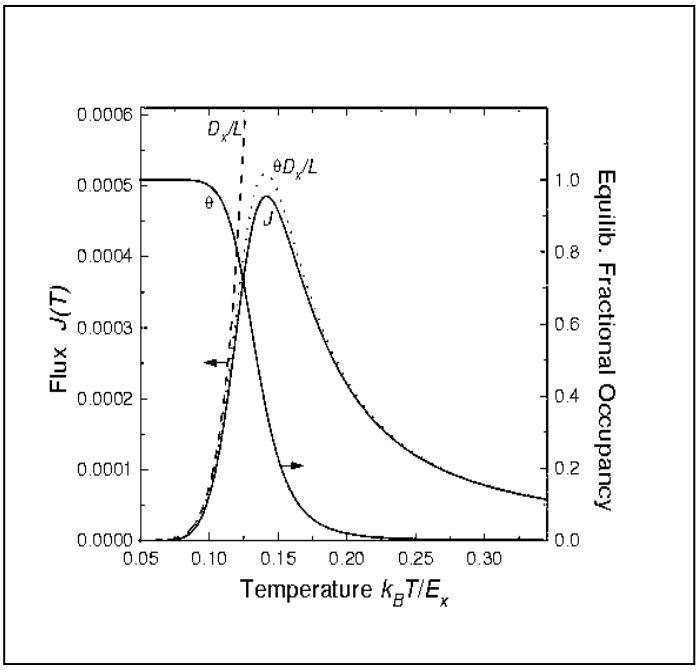


Figure 5: Temperature dependence of membrane flux and equilibrium fractional occupancy for single-component permeation through Langmuirian membranes.

low temperatures, because of increasing the likelihood of surmounting site-to-site barriers. At higher temperatures, though, the flux decreases with temperature (at fixed pressure) because adding heat decreases the fractional loading, hence decreasing the density factor in equation (1), i.e., "flux = density × velocity." A third regime of flux vs. temperature has been reported in zeolite membrane permeation measurements, which became the focus of discussion at the NATO-ASI. In particular, at very high temperatures the flux is seen to increase again with temperature, albeit very weakly [18-20]. This may be attributed to populating high-energy, non-zeolitic permeation pathways (cf. dusty gas model [21-23]), or to the onset of flow within zeolite pores. Both are possible, although the latter hypothesis stretches credulity a bit.

## 3. Temperature and Loading Dependencies of Diffusion Coefficients:

In section 2 we developed the phenomenologies underlying the Fickian, self and Maxwell-Stefan diffusion coefficients. In what follows, we assume diffusion-limited transport. We now discuss useful "rules of thumb" for how these diffusivities depend on temperature and loading. To understand how jump-like motion influences these dependencies, we also discuss the $T$- and $\theta$-dependencies arising from fluid-like intrapore motion, for comparison purposes. We begin by discussing temperature dependencies for fixed loading.

### 3.1. Temperature Dependence

Temperature has a strong influence on the jump diffusion process because of the increased likelihood of surmounting large energy barriers. This is usually expressed through the Arrhenius-type temperature dependence:

$$D_s \propto e^{-E_{act}/k_B T} \tag{23}$$

which arises from transition state theory (TST) for the site-to-site jump rate, according to:

$$k_{hop}^{TST} = \left[ \frac{\omega(T)}{2\pi} e^{\Delta S(T)/k_B} \right] . e^{-\Delta E(T)/k_B T} \tag{24}$$

where $T$ is temperature, $k_B$ is Boltzmann's constant, $\omega(T)$ is the temperature-dependent site vibrational frequency, $\Delta S(T)$ is the temperature-dependent activation entropy, and $\Delta E(T)$ is the temperature-dependent activation energy. Temperature ranges for which $\Delta E(T)/k_B T \gg 1$ give jump-like motion, rendering the pre-exponential factor in square brackets relatively weakly varying with temperature. The same qualitative form holds for the Fickian and Maxwell-Stefan diffusivities, although the apparent activation energy for these is not necessarily the same as in self diffusion [24].

Alternatively, temperature ranges for which $\Delta E(T)/k_B T \ll 1$ may deviate from the Arrhenius temperature dependence. When energy barriers are small, which is typical of fluid-like intrapore motion, the temperature dependence is usually weaker, arising from the quantities in square brackets in equation (24). In this case non-monotonic temperature dependencies are possible. Such a situation has been predicted for ethane in (not-yet-synthesized) siliceous Linde type A zeolite (LTA), whose schematic structure is shown in Figure 6A. There exists a predicted temperature window (150-300 K) in which $D_{self}$ actually decreases with temperature, as shown in Figure 6B [25]. This was explained by noting that increasing temperature moves ethane away from window sites, which are potential minima, hence decreasing the rate of cage-to-cage motion and thus slowing diffusion.

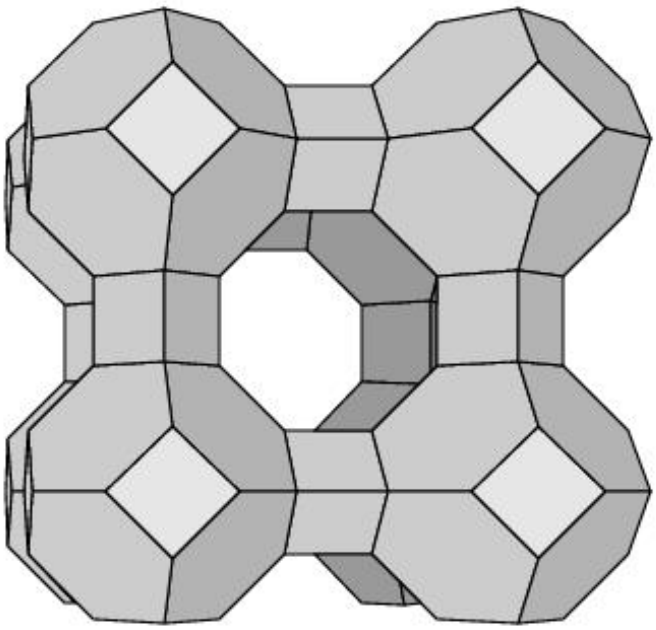

Figure 6A: Framework structure of siliceous LTA zeolite.

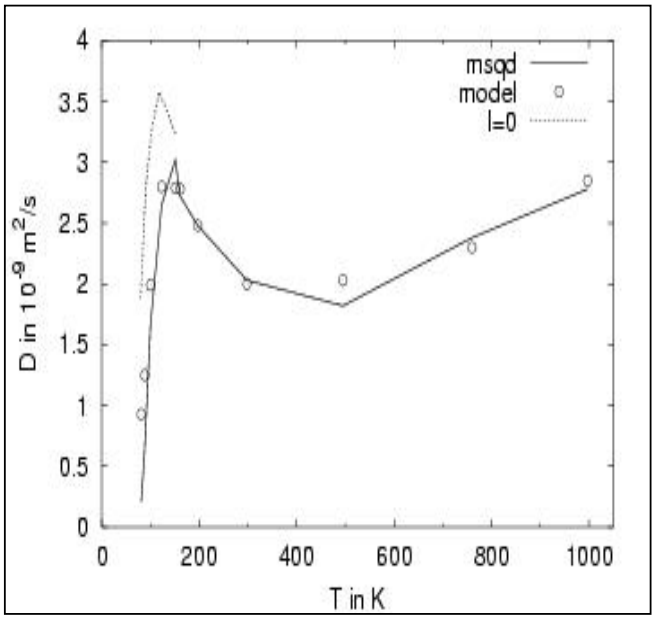


Figure 6B: Temperature dependence of the self-diffusivity of ethane at a loading of one molecule per cage.

3.2. Loading Dependence

Diffusion in zeolites is strongly influenced by guest-host and guest-guest interactions. The latter become manifest through loading dependencies of diffusion. NMR measurements have revealed five qualitatively different loading dependencies for intra-crystalline self diffusion [26]. The simplest of these, denoted type I, is monotonically decreasing and is characteristic of Langmuirian host-guest systems. Here, we explore Langmuirian loading dependencies of Self-, Maxwell-Stefan and Fickian diffusion coefficients for comparison with results arising from fluid-like motion. In our succeeding chapter in these Proceedings, we discuss systems that exhibit the other loading dependencies. The comparison is shown below in Table 1.

| CRITERION | JUMP DIFFUSION | FLUID-LIKE MOTION[11] |
|---|---|---|
| Isotherm (Langmuir) | $\Gamma = \frac{1}{1-\theta}$ | $\Gamma \approx \frac{1}{1-\theta}$ |
| Self-diffusivity | $D_s = D_0(1-\theta)f(\theta); f < 1$ | $D_s \approx D_0(1-\theta)$ |
| Maxwell-Stefan diffusivity | $D^{MS} = D_0(1-\theta)$ | $D^{MS} \approx D_0$ |
| Fick diffusivity | $D_{Fick} = D_0 = \text{constant}$ | $D_{Fick} = \frac{D_0}{(1-\theta)}$ |

**Table 1:** Comparison of loading dependencies of the Self-, Maxwell-Stefan and Fickian diffusivities for jump and fluid-like diffusive motion for Langmuirian host-guest systems.

In all cases the three diffusivities are equal to each other at the low-loading limit, i.e., at infinite dilution. The quantity $f(\theta)$ is called the vacancy correlation factor, is between 0 and 1 in all

cases, is equal to 1 at infinite dilution, and is discussed in more detail below. We note that mean-field theory of self diffusion is tantamount to setting $f(\theta) = 1$, which ends up giving the Maxwell-Stefan diffusivity for jump motion. This quantity is sometimes called the "jump diffusion coefficient," which seems less susceptible to vacancy correlations as compared to the self diffusivity. In all cases we see the relative trend $\boldsymbol{D}_{\text{Fick}} \geq \boldsymbol{D}^{\text{MS}} \geq \boldsymbol{D}_{\text{s}}$, where equality holds at infinite dilution. The loading dependencies for fluid-like motion were extracted from the seminal MD study by Maginn *et al*. on methane in silicalite [11]. Here we clearly see why the Maxwell-Stefan diffusivity is also called the "corrected diffusivity" [27], as the Fickian loading dependence is removed (corrected) by dividing $\boldsymbol{D}_{\text{Fick}}$ by $\boldsymbol{\Gamma}$.

## 4. Correlations and Correlation Functions:

### 4.1. Kinetic Correlations

We now discuss the correlations and correlation functions that form the language with which we understand diffusion in zeolites. We discuss here three different classes of correlations: kinetic, geometric and vacancy correlations. Kinetic correlations arise from slow thermalization of a molecule to its post-jump state. Kinetic correlations can be expressed through Newton's first law of motion applied to nanopore diffusion, given as: "A guest molecule in motion tends to remain in motion (until it bangs into a wall)." Consequences of kinetic correlations include: site-to-site jumps that are not nearest-neighbor jumps, i.e., multi-site jumps; and in the extreme case, mean-square displacements proportional to $t^2$ resulting in flow, i.e., ballistic-type of motion [28]. Kinetic correlations are more important at lower loadings and in channel-type zeolites rather than in cage-type zeolites.

4.2. Geometric Correlations

Geometric correlations arise from the anisotropic nature of many zeolite framework topologies. In the language of jump-diffusion, geometrical correlations arise when the sum of the jump vectors at a site does not vanish. Therefore, as observed for cation containing zeolites such as FAU (Figure 1) [29], molecules adsorbed at cation sites can jump away from cations but not into them, thereby producing geometric correlations that reduce the diffusion rate. However, when a molecule reaches a window site, these correlations are lost as the mean probability of jumping into the original cage or to the adjacent cage is the same. For channel-type zeolites such as ZSM-5 (Figure 1), geometric correlations arise for jumps from intersection sites but not from channel sites [30]. In such a situation, the channel geometry enables displacement in the z-direction only by sequential channel motions along the x- and y-directions. Based on this topology, a correlation rule has been proposed [30], which takes the following form when ignoring kinetic correlations (i.e., ignoring memory effects):

$$\frac{\boldsymbol{a}^2}{\boldsymbol{D}_s^x}+\frac{\boldsymbol{b}^2}{\boldsymbol{D}_s^y}=\frac{\boldsymbol{c}^2}{\boldsymbol{D}_s^z} \tag{25}$$

where a, b, c and $\boldsymbol{D}_s^x$, $\boldsymbol{D}_s^y$, $\boldsymbol{D}_s^z$ are the unit cell dimensions and self diffusivities in the x-, y- and z-directions, respectively. Some practical difficulties exist in testing this relation from experimental measurements due to the requirement of growing sufficiently large crystallites (in all directions) to obtain diffusivities in individual directions with reasonably good accuracy.

4.3. Vacancy Correlations

Vacancy correlations arise when the fractional loading is significantly greater than zero. Vacancy correlations can be expressed through Newton's second law of motion applied to

nanopore diffusion, given as: "A guest molecule in motion tends to return to its original site." In terms of jump-diffusion, a jump leaves behind a vacancy; thus, a molecule has a greater probability of returning to its original site (i.e., the vacancy) than it does to jump onward, thereby creating the opposite effect of kinetic correlations and decreasing diffusion coefficients. This effect is more important for lattices with low coordination [31] and at higher loadings.

Here we provide a more quantitative description of vacancy correlations, beginning with the Langmuirian model as described above. From Table 1 we recall the formula that defines the vacancy correlation factor:

$$\boldsymbol{D}_s(\theta) = \boldsymbol{D}_0(1-\theta)\boldsymbol{f}(\theta) \tag{26a}$$

A jump analysis of $\boldsymbol{f(\theta)}$ shows that [2]:

$$\boldsymbol{f}(\theta) = \frac{\left(1+\langle \cos\boldsymbol{\phi}\rangle\right)}{\left(1-\langle \cos\boldsymbol{\phi}\rangle\right)} \tag{26b}$$

where $\boldsymbol{\phi}$ is the angle between consecutive jumps. The molecular motion becomes clear by analyzing the extreme limits possible for $\langle \cos\boldsymbol{\phi}\rangle$. In particular, when $\langle \cos\boldsymbol{\phi}\rangle = -1$, the motion is purely vibrational, and the self diffusivity vanishes ($\boldsymbol{D_s} = 0$); while when $\langle \cos\boldsymbol{\phi}\rangle = +1$, the motion is purely ballistic (i.e., flow) and the self-diffusivity blows up ($\boldsymbol{D_s} = \infty$). Diffusion in zeolites is characterized by vacancy correlations in between these two extremes.

Single-file diffusion signifies motion where molecules diffuse in one-dimensional channels that are so narrow that larger molecules cannot pass each other, i.e., the ordering of molecules is preserved. Such strong confinement introduces particularly strong vacancy correlations. At short times ($\boldsymbol{t} < \boldsymbol{L}^2/\boldsymbol{D}_0$, where $\boldsymbol{L}$ is membrane thickness), these correlations qualitatively change the

behavior of mean-square displacements (MSD, see equation (15)), from $t$ to $t^{1/2}$ dependence. Such is an example of "anomalous" diffusion. At longer times, the linear time-dependence re-emerges, but with an anomalous self-diffusivity [13, 32]. This can be expressed through the vacancy correlation factor, which for single-file diffusion takes the form:

$$f(\theta) = \frac{1}{L\theta} \tag{26c}$$

Equation (26c) presents a rare example where a transport coefficient depends on macroscopic systems size. While we expect flux to depend on system size, especially for diffusion-limited transport, we usually expect the self diffusivity to be intensive, i.e., independent of system size. The long-time anomaly of single-file diffusion is thus manifested by a non-intensive diffusivity.

4.4. Correlation Functions

Having discussed the qualitative nature of correlations in jump diffusion, we now quantify them through statistical mechanical correlation functions. Under equilibrium conditions, i.e., without a chemical potential gradient, random sorbate motion is described by the self-diffusivity as defined in the Einstein equation:

$$\left\langle r^2(t) \right\rangle \equiv \left\langle \left| r(t) - r(0) \right|^2 \right\rangle \to 6D_s t \tag{27a}$$

$$\Rightarrow D_s = \frac{\left\langle r^2(t) \right\rangle}{6t} \tag{27b}$$

At a microscopic level, the self-diffusion coefficient is controlled by the motion of a *tagged* sorbate, possibly in the midst of identical untagged molecules. Equation (27b) can be recast in the form of a more traditional correlation function, a so-called Green-Kubo relation, which gives the diffusivity as the long-time integral of the velocity auto-correlation function:

$$\boldsymbol{D}_s = \int \boldsymbol{dt} \frac{\langle \boldsymbol{v}(0).\boldsymbol{v}(\boldsymbol{t}) \rangle}{3} \tag{28}$$

Equations (27b) and (28) thus provide two formally equivalent means for calculating $\boldsymbol{D}_s$, which turn out to have different regimes of practical application. Equation (27b) is useful for both jump diffusion and fluid-like motion, evaluated with kinetic Monte Carlo or molecular dynamics (MD), respectively. Alternatively, equation (28) is only useful for treating fluid-like motion, which is typically modeled using MD. This is because in fluid-like motion, velocity correlations decay on time scales comparable to those that control diffusion. On the other hand, in jump diffusion, velocity correlations typically decay well before rare jumps occur, making equation (28) less useful for diffusion, but still useful for revealing low-frequency vibrational motion at adsorption sites.

By studying mean-square displacements we can reveal the origin of the linear time dependence expected for diffusion. This is most conveniently expressed as motion on a lattice of sites. After n hops, the MSD takes the form:

$$\left\langle \boldsymbol{r}^2(\boldsymbol{n}) \right\rangle = \left\langle \left| \sum_i \boldsymbol{l}_i \right|^2 \right\rangle \tag{29a}$$

$$= \left\langle \sum_i \left| \boldsymbol{l}_i \right|^2 \right\rangle + \left\langle \sum_{i,j} \boldsymbol{l}_i \boldsymbol{l}_j \right\rangle \tag{29b}$$

$$= \boldsymbol{n} \left\langle \boldsymbol{a}^2 \right\rangle \quad + \text{ kinetic/geometric/vacancy correlations.} \tag{29c}$$

The second term in equation (29c) contains all the correlations discussed above, and indeed, takes the form of a jump-vector auto-correlation function. For a single random walker on a Langmuirian lattice, this second term identically vanishes. Expressing this ideal case in the language of an average jump time: $\boldsymbol{\tau} = \boldsymbol{t}/\boldsymbol{n}$ and thus $\boldsymbol{n} = \boldsymbol{t}/\boldsymbol{\tau}$, we find that:

$$\left\langle r^2(n)\right\rangle = \left(\frac{t}{\langle\tau\rangle}\right)\left\langle a^2\right\rangle \equiv 6D_s t \tag{29d}$$

$$\Rightarrow D_s = \frac{\left\langle a^2\right\rangle}{6\langle\tau\rangle} = k_{hop}\left\langle a^2\right\rangle \tag{29e}$$

Equation (29d) shows that the MSD is linear in time when the first term in equation (29b) dominates over the second term, even when the second term does not vanish. And equation (29e) shows how the self-diffusivity can be related to fundamental length and time scales. For more complex host-guest systems, such a transparent relationship between the self-diffusivity and fundamental system parameters may not be possible.

In Figure 7 we show a schematic MSD characteristic of diffusion in cage-type zeolites.

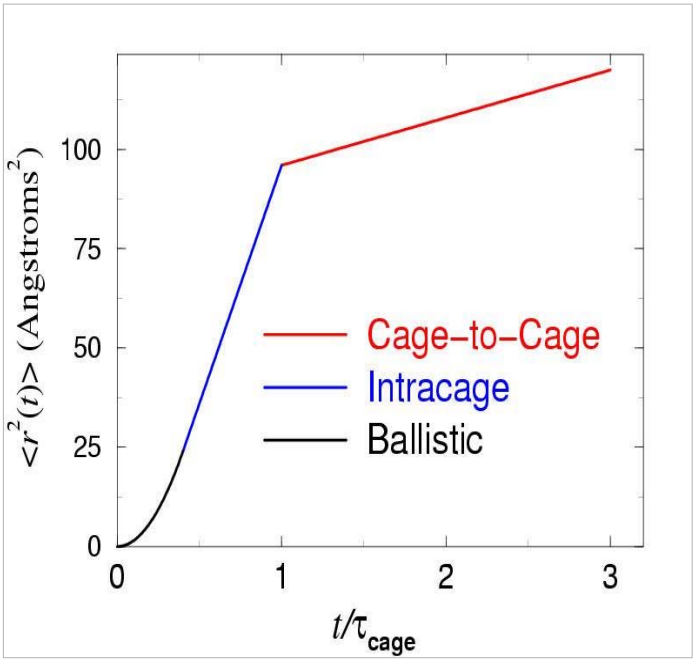


Figure 7: Typical mean-square displacement (MSD) plot for molecular motion in cage-type zeolites.

Two important transitions warrant comment in Figure 7. First, at short times, the MSD changes from ballistic ($t^2$) to diffusive ($t$) motion, as host-guest and guest-guest collisions randomize molecular motion. This transition usually occurs at very short times, on the order of picoseconds or less. At longer times, the MSD changes from intrapore motion (diffusive with larger slope) to cage-to-cage motion (diffusive but with smaller slope). Modelers must be careful to ensure that MSD slopes actually represent cage-to-cage motion; otherwise, self-diffusivities so obtained are not comparable with results from, e.g., pulsed field gradient NMR data.

While self-diffusion probes motion of individual, tagged particles, correlation functions relevant to Fickan and Maxwell-Stefan diffusivities involve cooperative motion, i.e., correlations between different sorbates and even components in the system. The relevant correlation functions are shown below in Table 2 for single-component diffusion systems. In Table 2 below, we see clearly that the Maxwell-Stefan diffusivity augments the self-diffusivity with correlations between different sorbate molecules. This is ironic because from analysis above, we found that the

| SELF-DIFFUSION | MAXWELL-STEFAN DIFFUSION$^{\Psi}$ |
|---|---|
| $D_s = \int dt \frac{\langle v(0).v(t) \rangle}{3}$ <br> $= \sum_i \int dt \frac{\langle v_i(0).v_i(t) \rangle}{3n}$ | $D^{MS} = \sum_{i,j} \int dt \frac{\langle v_i(0).v_j(t) \rangle}{3n}$ <br> $= D_s$ + $i$-$j$ velocity correlations <br> $= \sum_{i,j} \frac{\langle [r_i(t) - r_i(0)].[r_j(t) - r_j(0)] \rangle}{6nt}$ |

**Table 2:** Correlation functional relations for the Self- and Maxwell-Stefan diffusivities for single component diffusive motion.

Maxwell-Stefan diffusivity is less susceptible to vacancy correlations than is the self-diffusivity. Thus, the additional ***i-j*** correlations present in the Maxwell-Stefan diffusivity must somehow wash out vacancy correlations. Similar expressions can be written for multi-component systems as well [33, 34].

## 5. Interactions and Rare-Event Simulations:

### 5.1. Potential Energy

Underlying these correlation functions is the total potential energy of the host-guest system, $V$, which consists of the following terms:

$$V = V_H + V_G + V_{HG} + V_{GG}, \tag{30}$$

where $V_H$ and $V_G$ are the host and guest distortion energies, respectively; and $V_{HG}$ and $V_{GG}$ are the host-guest and guest-guest interaction energies, respectively. Detailed forms for each of these terms are offered by Snurr in his chapter in these Proceedings. Each of these terms can play an important role for modeling jump diffusion in zeolites. Due to computational complexity, most such simulations have been performed at infinite dilution, where $V_{GG} = 0$. Furthermore, many jump diffusion simulations have assumed that the zeolite remains rigid ($V_H \equiv 0$), and some even assume that the guest remains rigid ($V_G \equiv 0$), leaving only the host-guest interaction. To be sure, this is the most important starting point for modeling diffusion in zeolites, but future studies must reckon with these other interactions. In particular, in the succeeding chapter to this one, we touch on recent studies that include $V_H$ and $V_{GG}$ for modeling framework flexibility and many-sorbate effects, respectively.

---

[Ψ] Here, ***i*** and ***j*** represent different molecules of the same component

5.2. Transition State Theory

Having formulated the potential energy function, transition state theory (TST) calculations can be performed to predict site-to-site jump rate coefficients for a given host-guest system. The TST approximation can be formulated for gas phase as well as condensed phase systems using classical or quantum mechanics. In general, one considers a jump from a "reactant" state (A) to a "product" state B through a transition state (TS), which is the first-order saddle point connecting states A and B. Figure 8A shows a well-studied example: benzene in Na-Y jumping from a cation site (A) to a window site (B). The general potential energy map associated with such a jump is shown in Figure 8B. The standard procedure in TST is to replace the net flux from reactants to products with the instantaneous flux through the transition-state dividing surface. Using this idea, the TST rate constant is given by [1]:

$$k_{A\to B}^{TST} \approx \sqrt{\frac{k_B T}{2m\pi}} \times \frac{Q_{TS}}{Q_A} \tag{31}$$

where $m$ is the reduced mass associated with the reaction coordinate; and $Q_A$ and $Q_{TS}$ are the configurational partition functions for the reactant and transition state, respectively. These partition functions are usually calculated using specialized Monte Carlo methods [1]. The great challenge in all TST calculations is locating the transition state and mathematically formulating the dividing surface. When one has an educated guess regarding the reaction coordinate $x$, but no knowledge of the transition state or the dividing surface, a reliable but computationally expensive solution is to

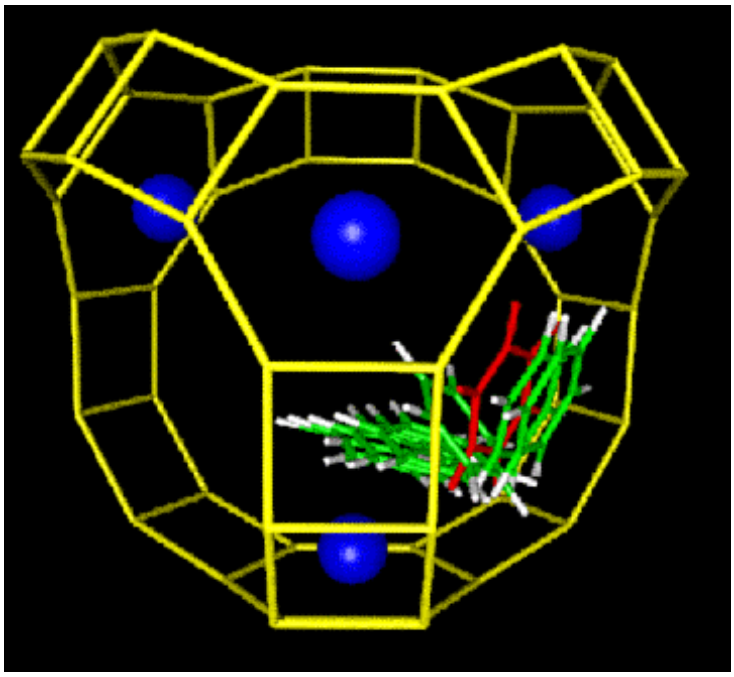

Figure 8A: Transition state theory approximation for jump-diffusion in cage-type zeolites: Example of a site-to-site jump in a FAU supercage.

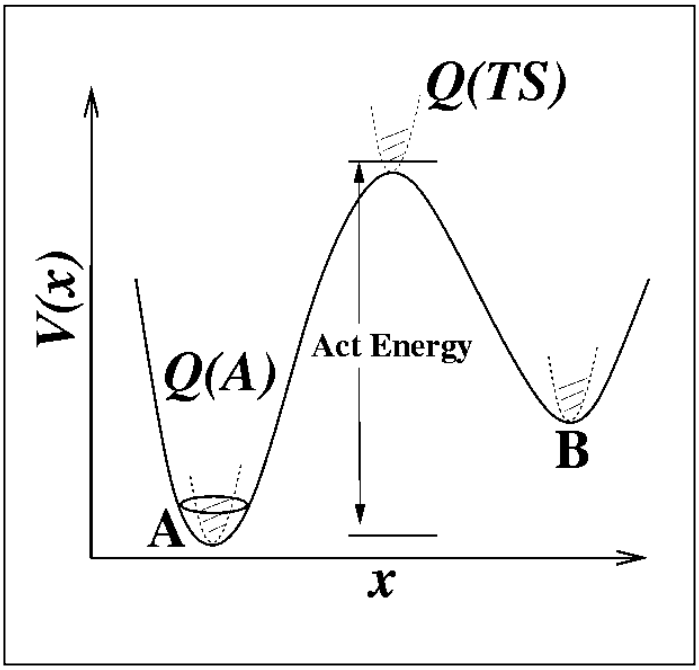


Figure 8B: Transition state theory approximation for jump-diffusion in cage-type zeolites: Potential energy diagram illustrating that the jump in Figure 8A progresses with an activation energy barrier across the transition state.

calculate the free energy surface ***F(x)***, also known as the potential of mean force or the reversible work surface. Here $exp[-\boldsymbol{F}(\boldsymbol{x})/\boldsymbol{k}_B\boldsymbol{T}]$ is proportional to the probability that the reaction coordinate takes the value ***x***, while all other coordinates are Boltzmann-averaged at temperature ***T***. The TST rate constant can then be rewritten as:

$$\boldsymbol{k}_{A\to B}^{TST} \approx \sqrt{\frac{\boldsymbol{k}_B\boldsymbol{T}}{2\boldsymbol{m}\boldsymbol{\pi}}} \times \frac{\boldsymbol{e}^{-\frac{F(TS)}{k_BT}}}{\int_A \boldsymbol{e}^{-\frac{F(x)}{k_BT}}\boldsymbol{dx}} \tag{32}$$

The free energy surface can often be calculated from the same specialized Monte Carlo methods used to compute partition functions.

The basic TST approach works well when the correct dynamical bottleneck(s) can be located. However, transition state searches are often launched by intuition; what can we do when our intuition fails? Two important methods come to the rescue, both pioneered by Chandler and coworkers [1, 35]. When a reasonable estimate of the transition state is available, but little knowledge of the dividing surface is at hand, we recommend performing reaction flux correlation function calculations [36]. This approach involves running a swarm of very short MD trajectories from a putative dividing surface to calculate the fraction that actually react, the so-called transmission coefficient, $\boldsymbol{\kappa}$. If $\boldsymbol{\kappa}$ is of order unity, the putative transition state and the dividing surface are close to the actual ones. Alternatively, if $\boldsymbol{\kappa}$ is much less than unity, then either the transition state and/or the dividing surface are in error, indicating that mechanistic knowledge about the jump process is lacking. Unfortunately, the reactive flux correlation function approach will not provide such understanding.

To obtain better mechanistic knowledge, we recommend performing transition path sampling calculations [37, 38]. This approach is the *cadillac* of reaction dynamics methods, requiring no knowledge of a transition state or dividing surface. The transition path approach involves a Monte Carlo sampling of paths that connect reactant and product in time $t$, and using this information to build a statistical ensemble of transition states, which is tantamount to the dividing surface. This should be the last resort, because it is rather computationally demanding.

5.3. Kinetic Monte Carlo

Armed with the rate coefficients for site-to-site jumps in a zeolite, we have much information about motion, but still no diffusion coefficient. The link between the two is provided by kinetic Monte Carlo (KMC) simulations [1], which can be thought of as spatially discrete MD calculations that evolve the lattice model in time. KMC can be used to compute ensemble averages, correlation functions, and most important to us, mean-square displacements. Input to KMC includes the lattice connectivity, initial site occupancies, and all the site-to-site rate coefficients. While this list seems short, imagining and simulating all possible jumps can still be daunting. KMC can account for complex lattices with many site types; adsorption/desorption and reactive events; kinetic, geometric and vacancy correlations; single-file diffusion; and guest-guest attractions. On the other hand, KMC fails to account for processes we did not think of, off-lattice motion (i.e., fluid-like motion), and complex cooperative dynamics such as polymer relaxation.

Descriptions for how to implement KMC can be found in the recent literature [1, 2]. In general, one can use fixed for variable time steps. The fixed time-step method is simple, easy to implement, and convenient for calculating time correlation functions. However, it becomes inefficient for systems with many time scales, i.e., when rate coefficients span many orders of magnitude. In this case, the variable time-step method becomes useful. Although it is more

complicated to use this approach for computing time correlation functions, it remains relatively simple to evaluate mean-square displacements using the variable time-step approach. In this case the probability to make a jump is proportional to the rate coefficient for that jump, and the system time elapsed prior to the jump is the inverse of the sum of rates for all available jump processes for that configuration.

## V. Concluding Remarks

We have reviewed the basic principles and methodologies involved in understanding jump diffusion in zeolites. We focused on single-component diffusion, and explored the Fickian and Maxwell-Stefan approaches for modeling this phenomenon. We emphasize that while the Fickian approach is more convenient for Langmuirian systems, the Maxwell-Stefan approach is clearly advantageous for realistic modeling of multi-component adsorbed phase diffusion, hands down! We discussed expected temperature and loading dependencies of diffusion, and how these are influenced by various correlations in the system. Finally, we touched on modern methods for simulating jump diffusion in zeolites; these methods will be brought to life in our succeeding chapter dealing with applications of these ideas. Overall, we hope that our main point has gotten across – that diffusion in zeolites can be elucidated by thinking in terms of sites, lattices, jumps and in general, rare events. Thank you. Applause.

**Acknowledgments:**

SMA would like to gratefully acknowledge NATO and the UMass Amherst Office of Research Affairs for funding SMA's attendance at the NATO ASI. SMA also gratefully acknowledges generous funding from the National Science Foundation (NSF) supporting the

group's research on modeling jump diffusion in zeolites. RH would like to acknowledge Prof. Michael Tsapatsis for guidance in dissertation research; the National Environmental Technology Institute; and NSF NIRT grant (CTS-0103010) for supporting research on zeolites.

References:


1. Auerbach, S.M., *Theory and simulation of jump dynamics, diffusion and phase equilibrium in nanopores.* International Reviews in Physical Chemistry, 2000. **19**(2): p. 155-198.
2. Karger, J., S. Vasenkov, and S.M. Auerbach, *Diffusion in zeolites*, in *Handbook of Zeolite Science and Technology*, P.K. Dutta, Editor. 2003, Marcel-Dekker: New York. p. 928.
3. Xomeritakis, G., et al., *Growth, microstructure, and permeation properties of supported zeolite (MFI) films and membranes prepared by secondary growth.* Chemical Engineering Science, 1999. **54**(15-16): p. 3521-3531.
4. Nair, S. and M. Tsapatsis, *Synthesis and properties of zeolite membranes*, in *Handbook of Zeolite Science and Technology*, P.K. Dutta, Editor. 2003, Marcel-Dekker: New York. p. 928.
5. Lai, Z.P., et al., *Microstructural optimization of a zeolite membrane for organic vapor separation.* Science, 2003. **300**(5618): p. 456-460.
6. Krishna, R., *Problems and pitfalls in the use of the fick formulation for intraparticle diffusion.* Chemical Engineering Science, 1993. **48**(5): p. 845-861.
7. Nelson, P.H. and J. Wei, *A theory for two-component diffusion in zeolites.* Journal of Catalysis, 1992. **136**(1): p. 263-266.
8. Karger, J. and D. Ruthven, *Diffusion in zeolites and other microporous solids*. 1992, New York: Wiley.
9. Sanborn, M.J. and R.Q. Snurr, *Predicting membrane flux of $CH_4$ and $CF_4$ mixtures in faujasite from molecular simulations.* Aiche Journal, 2001. **47**(9): p. 2032-2041.
10. Krishna, R., *Modeling issues in zeolite applications*, in *Handbook of Zeolite Science and Technology*, P.K. Dutta, Editor. 2003, Marcel-Dekker: New York. p. 928.
11. Maginn, E.J., A.T. Bell, and D.N. Theodorou, *Transport diffusivity of methane in silicalite from equilibrium and non-equilibrium simulations.* Journal of Physical Chemistry, 1993. **97**(16): p. 4173-4181.
12. Nelson, P.H. and S.M. Auerbach, *Modeling tracer counter-permeation through anisotropic zeolite membranes: from mean field theory to single-file diffusion.* Chemical Engineering Journal, 1999. **74**(1-2): p. 43-56.
13. Nelson, P.H. and S.M. Auerbach, *Self-diffusion in single-file zeolite membranes is Fickian at long times.* Journal of Chemical Physics, 1999. **110**(18): p. 9235-9243.
14. Saravanan, C. and S.M. Auerbach, *Theory and simulation of cohesive diffusion in nanopores: Transport in subcritical and supercritical regimes.* Journal of Chemical Physics, 1999. **110**(22): p. 11000-11011.
15. Sholl, D.S. and K.A. Fichthorn, *Concerted diffusion of molecular clusters in a molecular sieve.* Physical Review Letters, 1997. **79**(19): p. 3569-3572.
16. Kutner, R., *Chemical diffusion in the lattice gas of non-interacting particles.* Physics Letters A, 1981. **81**(4): p. 239-240.
17. Nelson, P.H., M. Tsapatsis, and S.M. Auerbach, *Modeling permeation through anisotropic zeolite membranes with nanoscopic defects.* Journal of Membrane Science, 2001. **184**(2): p. 245-255.
18. Bakker, W.J.W., et al., *Temperature dependence of one-component permeation through a silicalite-1 membrane.* Aiche Journal, 1997. **43**(9): p. 2203-2214.
19. Bakker, W.J.W., et al., *Permeation characteristics of a metal-supported silicalite-1 zeolite membrane.* Journal of Membrane Science, 1996. **117**(1-2): p. 57-78.
20. Xiao, J.R. and J. Wei, *Diffusion mechanism of hydrocarbons in zeolites .1. Theory.* Chemical Engineering Science, 1992. **47**(5): p. 1123-1141.
21. Jackson, R., *Transport in porous catalysts*. 1977, New York: Elsevier Scientific Pub. Co. 197.

22. Mason, E.A. and A.P. Malinauskas, *Gas transport in porous media: The Dusty-gas model*. 1983, New York: Elsevier Scientific Pub. Co.,. 194.

23. Wesselingh, J.A. and R. Krishna, *Mass transfer*. 1990, Chichester, U.K.: Ellis Horwood Ltd. 243.

24. Harikrishnan, R., S.M. Auerbach, and M. Tsapatsis, *Manuscript in preparation.* 2003.

25. Schuring, A., et al., *On entropic barriers for diffusion in zeolites: A molecular dynamics study.* Journal of Chemical Physics, 2002. **116**(24): p. 10890-10894.

26. Karger, J. and H. Pfeifer, *Nmr self-diffusion studies in zeolite science and technology.* Zeolites, 1987. **7**(2): p. 90-107.

27. Ruthven, D.M., *Principles of adsorption and adsorption processes*. 1984, New York: Wiley-Interscience. 433.

28. Skoulidas, A.I., et al., *Rapid transport of gases in carbon nanotubes.* Physical Review Letters, 2002. **89**(18): p. art. no.-185901.

29. Jousse, F., S.M. Auerbach, and D.P. Vercauteren, *Correlation effects in molecular diffusion in zeolites at infinite dilution.* Journal of Chemical Physics, 2000. **112**(3): p. 1531-1540.

30. Karger, J., *Random-walk through two-channel networks - a simple means to correlate the coefficients of anisotropic diffusion in ZSM-5 type zeolites.* Journal of Physical Chemistry, 1991. **95**(14): p. 5558-5560.

31. Coppens, M.O., A.T. Bell, and A.K. Chakraborty, *Effect of topology and molecular occupancy on self-diffusion in lattice models of zeolites - Monte-Carlo simulations.* Chemical Engineering Science, 1998. **53**(11): p. 2053-2061.

32. Hahn, K. and J. Karger, *Deviations from the normal time regime of single-file diffusion.* Journal of Physical Chemistry B, 1998. **102**(30): p. 5766-5771.

33. Theodorou, D.N., R.Q. Snurr, and A.T. Bell, *Molecular dynamics and diffusion in microporous materials*, in *Comprehensive supramolecular chemistry*, J.L.A.e. al.], Editor. 1996, Pergamon Press: New York. p. 507-548.

34. Tepper, H.L. and W.J. Briels, *Comments on the use of the Einstein equation for transport diffusion: Application to argon in AlPO4-5.* Journal of Chemical Physics, 2002. **116**(21): p. 9464-9474.

35. Chandler, D., *Statistical-mechanics of isomerization dynamics in liquids and transition-state approximation.* Journal of Chemical Physics, 1978. **68**(6): p. 2959-2970.

36. Jousse, F. and S.M. Auerbach, *Activated diffusion of benzene in NaY zeolite: Rate constants from transition state theory with dynamical corrections.* Journal of Chemical Physics, 1997. **107**(22): p. 9629-9639.

37. Vlugt, T.J.H., C. Dellago, and B. Smit, *Diffusion of isobutane in silicalite studied by transition path sampling.* Journal of Chemical Physics, 2000. **113**(19): p. 8791-8799.

38. Dellago, C., et al., *Transition path sampling and the calculation of rate constants.* Journal of Chemical Physics, 1998. **108**(5): p. 1964-1977.